PCCP

Cite this: *Phys. Chem. Chem. Phys.*, 2012, **14**, 9050–9053

www.rsc.org/pccp

COMMUNICATION

On the controversy of metal ion composition on amine oxygenase (AurF): a computational investigation†

Prabha Jayapal* and Gopalan Rajaraman*

Received 20th March 2012, Accepted 11th May 2012
DOI: 10.1039/c2cp40874k

An energetics–spectroscopic approach based on DFT method reveals that the active site structure of AurF has $\{Fe^{III}_2O\}$ central core with one protonated terminal glutamate.

Metal ions play a vital role in the structure and unique property of the metalloenzymes.[1] The replacement of one metal ion with another will lead to the loss of their function, especially their redox properties.[1] Metal ions such as Fe and Mn exhibit dual nature by which the di-iron enzyme can often take up the manganese atom in the place of iron.[2,3] The bimetallic enzyme AurF[4] catalyzes the sequential oxidation of aminoarenes to nitroarenes in the biosynthesis of the antibiotic aureothine (Fig. 1a).[2] This enzyme has gathered the attention of the scientific community due to the controversy on the nature of the metal ions present in the active centre.[2] Based on several experimental and spectroscopic techniques[4–6] three different metal compositions Fe–Fe,[4] Mn–Mn[5] and a mixed Mn–Fe[6] have been proposed.

EPR and Mössbauer spectroscopic (MB) data on AurF[4,6,7] provide two different perspectives on the metal ion composition. The EPR spectrum of the resting state of AurF resembles a Mn–Fe enzyme[7] and this leads to the proposal of a Mn–Fe composition for AurF. On the other hand, ICP (inductively coupled plasma atomic emission spectrometry), EPR of one electron reduced Fe^{II}–Fe^{III} form and accurate MB measurements indicate a di-iron composition for AurF.[4,7] Besides, the X-ray crystal structure of AurF has been independently solved by two groups claiming Fe–Fe[1b] and Mn–Mn[5b] compositions. A combined biochemical, structural and catalytic studies strongly favours a di-iron form with the Mn ion being an external impurity.[4b] Additionally trapping of a long-lived peroxodiiron(III) species during the catalytic cycle of AurF authenticates the presence of di-iron in its active form.[4a,c] Despite numerous experimental and spectroscopic studies on AurF, still no consensus on the metal ion composition has emerged.[4c]

Nowadays quantum chemical methods are widely used to determine the electronic structures of metalloenzyme and provide significant insight into the system with respect to the structure energies and spectral properties.[9] Apart from structure and energetics, the quantum chemical methods are also widely used to compute accurately the spectroscopic parameters.[8–10] In this contribution, we report the first theoretical investigation on the AurF enzyme by attempting to shed-light on the metal ion composition by computing geometries, electronic structure, energetics and most importantly the spectroscopic parameters for different models of AurF. As experimental data are available for both the Fe^{III}–Fe^{III} and Fe^{II}–Fe^{III} forms,[7] computation has been performed on both the species for clarity. Six sets of models having the core structure of (i) $\{Fe_2^{III}O\}$ (*M*1) (ii) $\{Mn^{III}OFe^{III}\}$ (*M*2) and (iii) $\{Fe_2^{II/III}O\}$ (*M*3) and their μ–OH protonated counter parts (*M*1*p*, *M*2*p* and *M*3*p*) haven been modelled. Due to the ambiguity[4b,11] on the protonation of two terminal glutamate residues (GLU 196 and GLU 277, numbered as per ref. 1*b*) at site 2 (see Fig. 1a), this set is expanded where these two glutamates are protonated independently and thus giving rise to a total of eighteen models; twelve oxidised and six mixed valance state models (see Fig. S1, ESI†). Note subscript 196 and 277 in front of M denotes its site 2 terminal glutamate protonation *e.g.*, models $_{196}M1$ and $_{267}M1$ denotes models with protonation at GLU 196 and GLU 267).

Optimised geometries and selected structural parameters of the computed models in comparison to the X-ray structure are

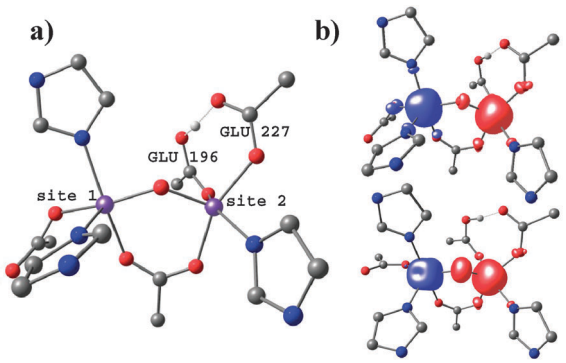

Fig. 1 (a) Active site model considered for investigation[1b] (optimized geometry of $_{196}M1$) (b) B3LYP computed spin density plots for models $_{196}M1$(top) and $_{196}M3$. The hydrogen atoms (except those involved in H-bonding) were omitted for clarity.

Department of Chemistry, Indian Institute of Technology-Bombay, Powai, Mumbai. E-mail: rajaraman@gmail.com, prabha.jaypal@gmail.com; Fax: +91-22-2572-3480; Tel: +91-22-2576-7183

† Electronic supplementary information (ESI) available: computational methodology, bond length, NSP, *J* values, MB parameters and EPR parameters of the models investigated, computed UV spectrum. See DOI: 10.1039/c2cp40874k

given in Fig. S1 and Table S1–S3 of the ESI.† In general, the M···M distances are slightly shorter for the μ-oxo structures (*M*1–*M*3) in comparison to the μ–OH counterparts (*M*1*p*–*M*3*p*) and the X-ray structure. This is consistent with the bond lengths reported for many di-iron model complexes.[9c,12] Our computed structures reveal that the glutamate 196 is unsymmetrically bound to the metal ion with one long and one short Fe–O_{glu} bond length (Fig. S1, ESI†). This is in agreement to the X-ray structure of AurF and other di-iron enzymes.[13] In general, model $_{196}M1$ structure resembles closely the X-ray active site (see Fig. S2 for overlay of two structures). Thus our calculations reveal that GLU 196 is likely to be protonated in the resting state of AurF and a similar conclusion has been derived based on DFT studies for the RNR enzyme.[14] Besides, in many of the protonated glutamate models, strong H-bonding interactions have been detected between two glutamate units (GLU 196 and 277) leading to the migration of a proton from one to another in some cases.[15] The tendency for protons to migrate to an area of high electron density has been observed earlier.[3,16] This tendency is expected for the resting state of AurF and the protonation state could be different during the catalytic cycle. Moreover, for models $_{227}M1p$, $_{227}M2p$ and $_{227}M3p$ there is also a strong hydrogen bonding interaction between GLU 227 and the μ-oxo bridging group. Such hydrogen bonding interactions are expected to adversely affect the spectral properties, particularly the magnetic coupling interactions (see Fig. S1, ESI†).[17] It is apparent that protonating GLU 196 or 277 leads to essentially isoenergetic structures with the computed energy difference being less than 1 kcal mol^{-1} (see Table S4, ESI†). On the other hand protonating the glutamate group of μ-OH models ($_{196}M2p$–$_{277}M2p$) adds a higher energy penalty as here the differences are as much as 3.5 kcal mol^{-1}. These differences in energetics arise mainly due to the conformational changes and hydrogen bonding interactions.

Due to subtle energy differences among the protonated models, the structure and energetics studies alone will not help to identify the metal ion composition. Thus, we have computed EPR and MB spectroscopic parameters on all the eighteen model complexes and absorption spectra in selected cases. Calculations have been performed with both hybrid B3LYP and pure BP86 functionals. The best suitable functional has been chosen based on the property of interest as reported earlier.[18] (see ESI for an elaborate discussion). In all the computed model complexes, an antiferromagnetic interaction between the metal ions has been noted leading to the stabilization of either doublet (for *M*2, *M*3) or a singlet (for *M*1) ground state. The computed NSP indicates that the metal–ligand covalency is correctly predicted (see Table 1, S5 and S6, ESI†). It is to be noted that the *M*1 models in general, provide a localized description compared to the *M*2 and *M*3 models. In models *M*2 and *M*3, significantly larger spin densities on the coordinating atoms including μ-oxo group have been observed. Besides, protonating the GLU 196 residue tends to increase the spin density on the μ-oxo group compared to GLU 227 protonated structures ($_{196}Mx$ *vs.* $_{277}Mx$ where x = 1, 2 and 3). This is because the GLU 227 protonated structures are involved in hydrogen bonding interaction with the μ-oxo group and this reduces significantly the spin density on this group.

The magnetic exchange interaction (*J*) is extremely sensitive to the small structural changes and this interaction is antiferromagnetic (AF) in all the computed cases, but the magnitude of *J* varies grossly across the series (see Table 1 and S7, ESI†). The computed values are in good accord to the experimentally reported values for the model complexes having $\{Fe^{III}_2O(OAc)\}$ core structures (J_{196M1} −194.6 *vs.* $J_{exp.}$ −234.4 cm^{-1}, see Fig. S2a, the reported complex is strikingly similar to the active site structure of AurF).[17] This variation in *J* is related to the magnitude of spin density found on the μ-oxo group of the high spin state (Table S7, ESI†). Upon protonation of the μ-oxo group, a significant reduction in the *J* values have been detected (*M*1*p* −47.2 cm^{-1}; $_{196}M1p$ −28.7 cm^{-1}). Although the *J* value has not been reported for this enzyme, the enzyme expressed in overabundance of iron is found to be EPR silent at 15 K.[77] Since no excited state signal has been detected at this temperature, the exchange interaction is likely to be strong[19] and this indirectly indicates that the core has μ–O rather than μ–OH which is in agreement to the computed *J* values. For *M*2 models, a slightly lower estimate of *J* has been observed compared to the corresponding *M*1 models (185 cm^{-1} *vs.* 133.6 cm^{-1} for *M*1 *vs.* *M*2). Like in *M*1, here also the protonation diminishes the *J* values significantly. The computed *J*s for the *M*3 models on the other hand are similar to that of *M*1 models (see Table S7, ESI†).

The MB spectrum of AurF has two isomer shifts (IS), one at 0.54 (δ_1) mm s^{-1} and another at 0.48 (δ_2) mm s^{-1}. Likewise, two quadrupolar splittings (QS), one at −1.86 mm s^{-1} and another at 0.80 mm s^{-1} have been observed (Table 1, S5 and S6, ESI†).[4a] The observance of two different IS and QS values suggest that the enzyme has two iron centres.[20] All the oxidized models (the *M*1 variations) have the δ values in the range of 0.5–0.6 mm s^{-1}. Quiet interestingly, the difference in δ values (δ_1–δ_2) observed experimentally is closer to that computed for *M*1 models. An unsymmetrical coordination environment between two iron sites (Fig. 1a) is the likely reason for the variation in IS and QS values. On the other hand, all the *M*2 and *M*2*p* models yield slightly larger δ values (δ > 6.0 mm s^{-1}). More apparent deviation with *M*2 models are in the estimate of QS, where relatively larger QS have been computed compared to the *M*1 variations. This mismatch clearly favours the di-iron composition for AurF. Within di-iron models, the $_{196}M1$ computed values resemble more closely the experiments (considering the magnitude and the sign of IS and QS values). Thus we propose that, $_{196}M1$ is likely to be the active site structure of AurF. Since experimental parameters are unavailable for the *M*3 state in AurF, we are comparing the computed values to the mixed valance form of uteroferrin[22] -another di-iron enzyme having structural resemblance to AurF. A variable oxidation state of the two sites leads to a large difference in the IS and QS values (higher δ_1–δ_2 and ΔE_{q_1}–ΔE_{q_2}) and this is nicely reproduced in the computed results (Table 1 and Table S6, better agreement is witnessed for $_{196}M3$, $_{277}M3$ models).

The oxidized Fe^{III}–Fe^{III} form with antiferromagnetic interaction will lead to a S = 0 ground state and is expected to be EPR silent. On the other hand, a mixed valent species has been detected in EPR, albeit with a weak signal intensity.[7] The EPR spectrum of the oxidized form grown in a Luria-Bertani medium however is distinctly different which is then simulated assuming a Mn^{III}–Fe^{III} composition to yield a set of g and A values

Table 1 Calculated and experimental[4,7,21] isomer shift δ (mm s^{-1}), quadrupole splitting ΔE_q (mm s^{-1}), hyperfine, g-tensor and Net Spin Population (NSP), and Heisenberg coupling constant J (cm^{-1}) of selected model complexes investigated

	$_{196}M1$	$_{196}M1p$	$_{196}M2$	$_{196}M2p$	Exp.[4,6,7,22]	$_{196}M3$	$_{196}M3p$
Net Spin Population							
NSP (Fe1) or (Mn1)	4.140	4.268	−3.822	−3.899		−3.721	−3.785
NSP (Fe2)	−4.169	−4.238	4.151	4.269		4.079	4.247
NSP(μ–O)	0.127	0.035	0.361	0.131		0.452	0.177
Heisenberg coupling constant							
J	−194.6	−28.7	−145.5	−24.6		−198.1	−15.4
EPR and Mössbauer parameters							
g-tensor	—	—	2.028, 2.057, 2.083	2.038, 2.046, 2.069	(2.030, 2.014, 2.015)[a] (1.94, 1.79, 1.70)[b]	1.906, 1.936, 1.952	1.882, 1.914, 2.045
Hyperfine Fe	—	—	−569, −606, −654	−624, −638, −641		−67, −70, −81	−71, −78, −88
Hyperfine Mn			213, 423, 656	167, 473, 512	210, 270, 322[a]	24, 78, 83	13,78, 85
δFe1/Mn1	0.602	0.592			0.54, 0.48		
δFe2	0.533	0.563	0.633	0.618	(1.24-Fe^{2+}, 0.53-Fe^{3+})[c]	0.969 0.640	0.713 0.839
ΔE_q Fe1/Mn1	0.926	0.830			−1.86, 0.80		
ΔE_q Fe2	−1.834	−1.075	−2.305	2.018	(+2.74-Fe^{2+} −1.93-Fe^{3+})[c]	2.248 −1.674	2.209 −3.786

[a] g and A values are obtained by simulating the EPR spectra assuming $Mn^{III}Fe^{III}$ composition.[6] [b] A rough estimation of g tensors reported for the mixed valent systems.[7] [c] Reported values for uteroferrin,[22] see text for details.

(see Table 1).[6] The estimated g tensors are nearly axial (2.03, 2.014 and 2.015) while the DFT computed values are rhombic in nature. Besides, the computed hyperfine interactions also strongly deviate from the experimental values. Moreover, calculations reveal a very large hyperfine tensor for Fe in the $M2$ series. All this basically indicates that, there is trace amount of manganese impurity which replaces the Fe leading to a Mn–Fe composition.[4b] Since the oxidized Fe^{III}–Fe^{III} form is EPR silent, even a trace amount of Mn can result in resolved EPR features. As the computed g and A tensors of $M2$ variants are largely different from that of experimental values, we believe that the active site structure could be significantly different from the one computed here. This is supported by the fact that, the presence of excess Mn leading to a dimanganese form losses its *in vivo* activity.[4b] Additionally the X-ray structure of the dimanganese form reveals that one of the terminal carboxylates undergoes the carboxylate shift where its coordination mode is transformed from the terminal to the bridging.[4b,5] Since accurate estimates of SH parameters for the mixed valence AurF are unavailable, comparison has been made to the structurally similar model complexes and a good agreement to both the g and A tensors has been observed.[22] We have also performed TD-DFT analysis on the $_{196}M1$ to complement the presented data. Experimental UV-vis spectroscopy[4a] reports a broad signal near 360 nm which is tentatively assigned to a oxo-to-iron charge transfer.

Our computed spectrum is shown in Fig. 2. The transitions at 312 and 355 nm are assigned as a charge transfer excitation with the first one being $d_{z^2} \rightarrow Op_z$ and the second one $d_{xz} \rightarrow Op_y$ transitions. Besides two weak transitions have also been observed at 408 and 562 nm and our analysis reveal that these are also ligand to metal charge transfer type transitions. In general, there is a good agreement between the computed and the experimental spectrum and this and all the data presented unequivocally support the $_{196}M1$ model as the active site structure for the AurF.

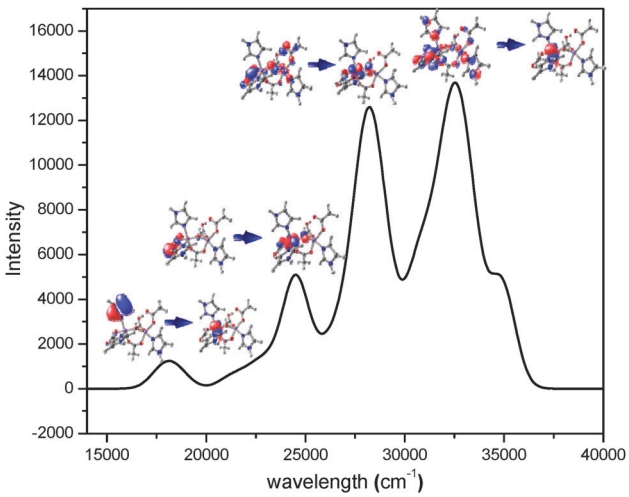

Fig. 2 TD-DFT calculated UV absorption spectrum of the model $_{196}M1$. See ref. 4*a* for the experimental spectrum. The contour plots of the orbitals corresponding to the excitation with the maximum oscillator strength are also shown.

To gain insight into the electronic structure of the active site of AurF, we have also performed MO analysis where we have plotted the α and β orbitals of $_{196}M1$ model (Fig. 3, S3). Due to the asymmetry of the coordinated ligand, the d-orbitals are split to a great extent compared to an ideal octahedral symmetry.

Although the d orbital ordering is the same for both α and β orbitals, the energy gap between the orbitals varies and this eventually leads to a difference in the IS/QS shift values. The metal orbitals have large ligand contributions indicating that there is large delocalization of spin density onto the ligands. Particularly, the μ-oxo group has large coefficients in both α and β orbitals and this eventually lead to a strong magnetic coupling.

In conclusion, we put forward in this communication the first and foremost initiative taken from the theoretical point of view to understand the structure–activity relationship of AurF enzyme.

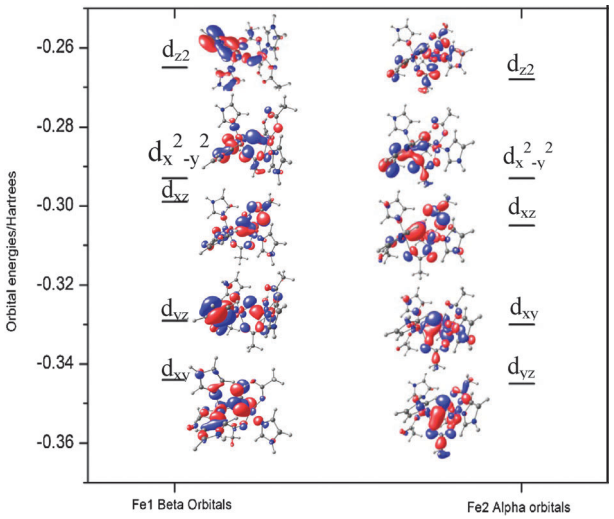

Fig. 3 Energies and the contour plot of the 3d orbitals of $_{196}M1$ model.

The structural and spectroscopic analysis broadly supports model $_{196}M1$ and $_{196}M3$ containing di-rion with a bridging μ-oxo and protonated GLU196 as the active site structure of the AurF in the oxidized and the mixed valent state.

PJ would like to thank DST-India for a FAST-TRACK young scientist fellowship (SR/FT/CS-56/2011). GR would like to acknowledge the DST (SR/S1/IC-41/2010) for funding and IIT-Bombay for computing facility.

Notes and references

1 (*a*) Q. Wang, J. E. Barclay, A. J. Blake, E. S. Davies, D. J. Evans, A. C. Marr, E. J. L. McInnes, J. McMaster, C. Wilson and M. Schröder, *Chem.–Eur. J.*, 2004, **10**, 3384; (*b*) T. Liu, B. Li, M. L. Singleton, M. B. Hall and M. Y. Darensbourg, *J. Am. Chem. Soc.*, 2009, **131**, 8296.
2 M. Carboni and J.-M. Latour, *Coord. Chem. Rev.*, 2011, **255**, 186.
3 (*a*) L. Capece, A. Lewis-Ballester, S.-R. Yeh, D. A. Estrin and M. A. Marti, *J. Phys. Chem. B*, 2012, **116**, 1401; (*b*) V. Mathrubootham, J. Thomas, R. Staples, J. McCraken, J. Shearer and E. L. Hegg, *Inorg. Chem.*, 2010, **49**, 5393.
4 (*a*) V. K. Korboukh, N. Li, E. W. Barr, J. M. Bollinger, Jr. and C. Krebs, *J. Am. Chem. Soc.*, 2009, **131**, 13608; (*b*) Y. S. Choi, H. Zhang, J. S. Brunzelle, S. K. Nair and H. Zhao, *Proc. Natl. Acad. Sci. U. S. A.*, 2008, **105**, 6858; (*c*) N. Li, V. N. Korboukh, C. Kerbs and J. M. Bollinger, Jr., *Proc. Natl. Acad. Sci. U. S. A.*, 2010, **10**, 15722.
5 G. Zocher, R. Winkler, C. Hertweck and G. E. Schulz, *J. Mol. Biol.*, 2007, **373**, 65.
6 C. Krebs, L. Matthews Megan, W. Jiang and J. M. Bollinger, Jr., *Biochemistry*, 2007, **46**, 10413.
7 M. Simurdiak, J. Lee and H. Zhao, *ChemBioChem*, 2006, **7**, 1169.
8 (*a*) W.-G. Han and L. Noodleman, *Dalton Trans.*, 2009, 6045; (*b*) C. More, V. Belle, M. Asso, A. Fournel, G. Roger, B. Guigliarelli and P. Bertrand, *Biospectroscopy*, 1999, **5**, S3.
9 (*a*) W.-G. Han and L. Noodleman, *Inorg. Chim. Acta*, 2008, **361**, 973; (*b*) S. Sinnecker, L. D. Slep, E. Bill and F. Neese, *Inorg. Chem.*, 2005, **44**, 2245; (*c*) P. Comba, L. R. Gahan, G. R. Hanson, V. Mereacre, C. J. Noble, A. K. Powell, I. Prisecaru, G. Schenk and M. Zajaczkowski-Fischer, *Chem.–Eur. J.*, 2012, **18**, 1700.
10 (*a*) W. A. Ames and S. C. Larsen, *J. Phys. Chem. A*, 2009, **113**, 4305; (*b*) J. F. Berry, E. Bill, E. Bothe, F. Neese and K. Wieghardt, *J. Am. Chem. Soc.*, 2006, **128**, 13515.
11 A. Ames, D. A. Pantazis, V. Krewald, N. Cox, J. Messinger, W. Lubitz and F. Neese, *J. Am. Chem. Soc.*, 2011, **133**, 19743.
12 D. M. KurtZ, Jr., *Chem. Rev.*, 1990, **90**, 585.
13 M. Strieker, E. M. Nolan, C. T. Walsh and M. A. Marahiel, *J. Am. Chem. Soc.*, 2009, **131**, 13523.
14 W. G. Han, D. A. Giammona, D. Bashford and L. Noodleman, *Inorg. Chem.*, 2010, **49**, 7266.
15 Our attempt to optimize a structure with μ–OH_2 bridging was unsuccessful as one of the proton is found to migrate to the GLU 277 residue.
16 R. Carrasco, I. Morgenstern-Badarau and J. Cano, *Chem. Commun.*, 2003, 436.
17 Yoon and S. J. Lippard, *J. Am. Chem. Soc.*, 2004, **126**, 2666.
18 (*a*) M. Römelt, S. Ye and F. Neese, *Inorg. Chem.*, 2009, **48**, 784; (*b*) P. Gasiorski, K. S. Danel, M. Matusiewicz, T. Uchacz, W. Kuźnik, Ł. Piątek and A. V. Kityk, *Mater. Chem. Phys.*, 2012, **132**, 330; (*c*) M. Radoul, M. Sundararajan, A. Potapov, C. Riplinger, F. Neese and D. Goldfarb, *Phys. Chem. Chem. Phys.*, 2010, **12**, 7276.
19 S. J. W. Holgate, G. Bondarenko, D. Collison and F. E. Mabbs, *Inorg. Chem.*, 1999, **38**, 2380.
20 Note: In protein environment having two asymmetric units, a slight variation among different units can also gives raise to two different values.
21 J. H. Rodriguez, H. N. Ok, Y. M. Xia, P. G. Debrunner, B. E. Hinrichs, T. Meyer and N. H. Packard, *J. Phys. Chem.*, 1996, **100**, 6849.
22 F. Li, M. Chakrabarti, Y. Dong, K. Kauffmann, E. L. Bominaar, E. Münck and L. Que Jr., *Inorg. Chem.*, 2012, **51**, 2917.